Targeting a single mismatched minor histocompatibility antigen with tumor-restricted expression eradicates human solid tumors

Lothar Hambach,[1] Marcel Vermeij,[2] Andreas Buser,[1] Zohara Aghai,[1] Theodorus van der Kwast,[2] and Els Goulmy[1]

[1]Department of Immunohematology and Blood Transfusion, Leiden University Medical Center, Leiden; and [2]Department of Pathology, Erasmus Medical Center, Rotterdam, The Netherlands

Regressions of metastatic solid tumors after allogeneic human leukocyte antigen (HLA)–matched stem cell transplantation (SCT) are often associated with detrimental graft-versus-host disease (GVHD). The graft-versus-host reaction of the HLA-matched donor is directed mainly against the multiple mismatched minor histocompatibility antigens (mHags) of the patient. mHags are strong HLA-restricted alloantigens with differential tissue distribution. Ubiquitously expressed mHags are the prime in situ targets of GVHD. The mHag HA-1 is hematopoiesis restricted, but displays additionally an aberrant expression on solid tumors. Thus, HA-1 might be an excellent target to boost the anti–solid tumor effect of allogeneic SCT without inducing severe GVHD. Here, we show that cytotoxic T lymphocytes (CTLs) solely targeting the human mHag HA-1 are capable of eradicating 3-dimensional human solid tumors in a highly mHag-specific manner in vitro, accompanied by interferon-γ release. In vivo, HA-1–specific CTLs distribute systemically and prevent human breast cancer metastases in immunodeficient mice. Moreover, HA-1–specific CTLs infiltrate and inhibit the progression of fully established metastases. Our study provides the first proof for the efficacy of a clinically applicable concept to exploit single mismatched mHags with hematopoiesis- and solid tumor–restricted expression for boosting the anti–solid tumor effect of allogeneic SCT. (Blood. 2008;112:1844-1852)

Introduction

Allogeneic human leukocyte antigen (HLA)–matched stem cell transplantation (SCT) is an established curative treatment for hematopoietic malignancies and an investigative immunotherapeutic approach for solid tumors. Initial trials of allogeneic SCT for advanced breast and renal cell cancer (RCC) showed encouraging results with regressions of widespread metastatic lesions. Some of these clinical responses were durable for more than 4 years.[1-6] Particularly in RCC, a disease hardly responding to chemotherapy, tumor regressions after allogeneic SCT were attributed to an immune-mediated graft-versus-tumor (GVT) effect. However, broad application of allogeneic SCT in solid tumor therapy remained limited due to the risk of severe graft-versus-host disease (GVHD) associated mostly with the GVT effects.[1-6] The major challenge for further improvements of stem cell (SC)–based allogeneic immunotherapy of solid tumors is therefore boosting specifically the GVT effect but not the GVHD immune reactivity.

The precise effector mechanisms of the GVT effect after HLA-matched allogeneic SCT are still unknown. The close association of clinical responses with GvHD suggests that the GVT effect is largely mediated by alloreactive T cells recognizing minor histocompatibility antigens (mHags) expressed on normal and malignant cells.[7] mHags are highly immunogenic polymorphic peptides presented in the context of HLA molecules. Despite HLA matching of donor and patient, mHag incompatibilities remain and result in strong donor T-cell responses against mHag alleles absent in the SC donor but present in the patient.[8] Due to the "allo-ness" of mHags, mHag-specific immune responses are not blunted by self-tolerance.[7] Thereby, allogeneic SCT overcomes a major limita-

tion of the commonly used cancer immunotherapies targeting autologous "tumor-associated antigens" (TAAs), where breaking self-tolerance remains an unsolved problem.[9] The key observation indicating that GVT effects can be separated from GVHD in humans was the finding that mHags display a differential tissue distribution. mHags are derived from genes that are either ubiquitously expressed or have a tissue-restricted expression.[10] We showed earlier that the ubiquitously expressed mHags are the prime in situ targets of GVHD.[11] Some hematopoiesis-restricted mHags are aberrantly expressed on solid tumor cells (so-called tumor mHags). The hematopoiesis-restricted mHag HA-1 is expressed on a broad spectrum of primary solid tumors, but not on normal nonhematopoietic tissue.[12,13] Moreover, HA-1–specific cytotoxic T lymphocytes (HA-1 CTLs) functionally recognize HA-1 on solid tumor cell lines in vitro.[12] Another known tumor mHag with HA-1–like characteristics is BCL2A1.[14] After HLA-matched allogeneic SCT, the patient's hematopoietic system is gradually replaced by the donor hematopoiesis, which is negative for the patient's hematopoiesis- and solid tumor–restricted tumor mHags. Thus, solid tumor cells remain the patient's only relevant tumor mHag$^+$ cells in the body, allowing highly selective targeting of cancer with tumor mHag CTLs.

Consequently, we suggested selective enhancement of the donor T-cell response against a single mismatched tumor mHag (such as HA-1) to boost the GVT effect with low risk of GVHD.[7] The goal of our study was to answer 2 core questions of our alloimmunotherapeutic concept. First, are CTLs directed at a single tumor mHag capable of eradicating human 3-dimensional (3D)

human tumors in a mHag-specific manner? Second, are CTLs targeting solely a single tumor mHag effective against human solid tumors in vivo? To answer these questions, we performed a detailed analysis of the efficacy of human HA-1 CTLs against human microtumors and explanted macroscopic tumors in vitro and against human macroscopic tumors and cancer metastases in translational animal models in vivo. We provide the first proof for the efficacy of the concept to eliminate cancer metastases by solely targeting mismatched tumor mHags.

Methods

Human cancer cell lines

The cancer cell lines MCF-7 and MDA-MB-231 (ATCC, Rockville, MD), 518A2 (kindly provided by Dr P. Schrier, Leiden University Medical Center), and BB65-RCC (kindly provided by Dr B. Van den Eynde, Ludwig Institute for Cancer Research, Brussels, Belgium) were genomically typed for the mHags HA-1 and H-Y by allele-specific polymerase chain reaction (PCR)[15] and analyzed for HA-1 mRNA expression as described.[12] Tumor cell lines were designated "HA-1$^+$," if positive for the immunogenic HA-1^H allele and for HA-1 mRNA.

Generation and culturing of HA-1– and H-Y–specific CTLs

The HA-1 CTL clones 1.7 and 2.12 were generated from peripheral blood mononuclear cells (PBMCs) of HLA-A2$^+$/HA-1^{RR} healthy donors as described.[16] Approval was obtained from the Leiden University Medical Center review board and informed consent was obtained in accordance with the Declaration of Helsinki. The HA-1 CTL clone 3HA15 and H-Y CTL clone 21-17 were isolated from patients after allogeneic SCT.[10,17]

Determination of cytotoxicity and IFN-γ release

Tumor cell killing by CTLs was tested in a standard 4-hour ^{51}Cr release assay as described.[16] IFN-γ concentrations were determined with the Pelikline enzyme-linked immunosorbent assay (ELISA) kit (CLB, Amsterdam, The Netherlands). Detection limit was 2 pg/mL.

Microtumor model

Microtumors in collagen matrix were generated according to a modified protocol[18] (L.H., E.G., manuscript in preparation). In brief, 6×10^4 tumor cells in 0.6 μL 3.65 mg/mL rat tail collagen type I (BD Biosciences Europe, Erembodegem, Belgium) were embedded between 2 layers of 50 μL collagen (base layer: 1.75 mg/mL, top layer: 1.31 mg/mL) and covered with 100 μL 20% human serum (HS) in IMDM (Invitrogen Life Technologies, Breda, The Netherlands). After 1 day, medium was replaced by 100 μL 20% HS in IMDM containing 240 IU/mL IL-2 (Chiron, Amsterdam, The Netherlands) and that was supplemented with CTLs or not. Microtumor growth was photographically documented at room temperature with an Axiovert 25 inverted microscope (Zeiss, Jena, Germany) using an A-Plan 2.5×/0.06 NA objective and a ProgRes C10 (Jenoptik, Jena, Germany) CCD camera. AxioVision 40 LE software (version 4.5; Zeiss, Sliedrecht, The Netherlands) was used for the control of image acquisition and for photograph analysis. Two-dimensional microtumor area ($\pi \times r1 \times r2$) was calculated after determination of the 2 maximal orthogonal microtumor radii r1 and r2. For histologic analysis, microtumors in collagen type I were fixed with 4% formalin for 24 hours at 4°C and embedded in paraffin as described in detail (L.H. and E.G., manuscript in preparation). H&E stainings were performed on 4-μm serial sections. Histologic analysis was performed by 2 independent pathologists.

Mouse models

Mice. Seven- to 11-week-old female nonobese diabetic/severe combined immunodeficient (NOD/scid) mice (Charles River, Lyon, France) were used. Experiments were performed after approval of the ethical committee of the Leiden University Medical Center.

Model of subcutaneous macrotumors. Mice were subcutaneously inoculated with 5×10^6 MDA-MB 231 cells in 200 μL IMDM with 1% FCS (Invitrogen Life Technologies). Human CTLs were quantified in peripheral blood samples and in organ and bone marrow suspensions by flow cytometry as described.[19]

Model of pulmonary microtumors. Mice were inoculated intravenously in a lateral tail vein with 5×10^5 or 7.5×10^5 MDA-MB 231 cells in 200 μL 1% FCS in IMDM and killed on day 40 or day 50, respectively. Lungs were inflated with 4% formalin via the trachea and fixed overnight at 4°C. Tumor nodules on the lung surface were quantified with a stereo dissecting microscope (Leica MZ 7.5; Rijswijk, The Netherlands). Serial sections (4 μm) were cut from paraffin-embedded right lung lobes. Intrapulmonal microtumors were counted after staining with antihuman cytokeratin antibodies.

Adoptive CTL transfer protocol. Mice were treated by intravenous administration of 3×10^7 CTLs in 200 μL 1% FCS in IMDM or with PBS as control as described.[20] All mice received 2×10^4 IU IL-2 intraperitoneally daily for 3 weeks.

Ex vivo tumor T-cell infiltration assay

Subcutaneously established tumors were explanted from untreated NOD/scid mice. Punch biopsies (3 mm in diameter) were sectioned horizontally at a height of 2 to 3 mm, placed on a transwell insert with 0.4-μm pore size (BD Biosciences, Franklin Lakes, NJ) of a 24-well plate, and demobilized with 100 μL rat tail collagen type I. Six hundred microliters 10% HS in IMDM with 120 IU IL-2 and 10^6 HA-1 CTLs were added to the insert and 1 mL 10% HS in IMDM with 120 IU IL-2 were added to the well. Medium was replaced every day. On day 3 after addition of CTLs, tumors in collagen type I were fixed with 4% formalin and 24 hours later embedded in paraffin.

Immunohistochemistry

Sections were stained with antihuman CD8 antibody (clone 4B11, dilution 1:20; Novocastra, Newcastle upon Tyne, United Kingdom) or pankeratin Ab-1 antibody (clone AE1/AE3, dilution 1/160; Labvision, Duiven, The Netherlands). Detection was performed with DAKO Envision Peroxidase/DAB kit (Dako, Heverlee, The Netherlands). Sections were counterstained with Mayer hematoxylin. Photographs were made at room temperature using an Axioskop 40 microscope (Zeiss) with A-Plan 5×/0.12 NA (only Figure 5B) or Plan-NeoFluar Oil 40×/1.3 NA (all other micrographs) objectives and captured with an AxioCam Mrc-5 CCD camera (Zeiss). Image acquisition was controlled by AxioVision 40 LE software.

Statistical Analysis

Different groups of mice were pairwise compared by a Mann-Whitney U test using SPSS 14.0 (SPSS, Chicago, IL). A P value less than .05 was considered statistically significant.

Results

HA-1 CTLs kill HA-1$^+$ solid tumor cells in vitro

To answer the question whether CTLs that direct a single tumor mHag are capable of clearing solid tumors in a mHag-specific manner, we selected a panel of solid tumor cell lines with differential molecular expression of the tumor mHag HA-1 and the ubiquitously expressed mHag H-Y for the subsequent experiments (Table S1; Figure S1A, available on the *Blood* website; see the Supplemental Materials link at the top of the online article). HA-1 and H-Y served as mutual controls for the mHag specificity of HA-1 or H-Y CTLs. Since recognition of the mHags HA-1 and H-Y by CTLs is HLA-A2 restricted, all selected tumor cell lines were HLA-A2$^+$. The expression levels of HLA-A2 differed
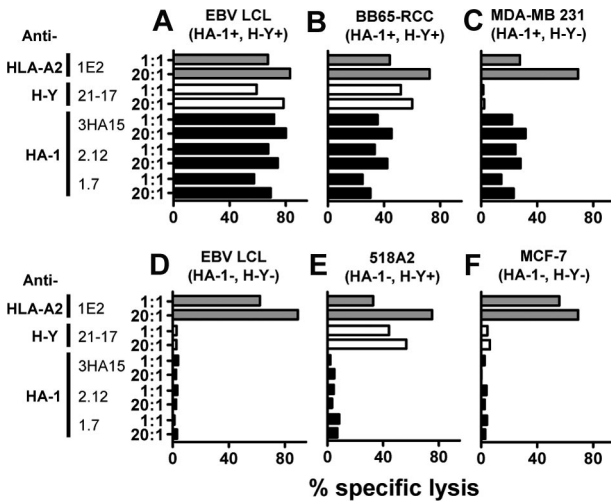
Figure 1. HA-1 CTLs lyse tumor cells in vitro. The in vitro killing efficacy of CTLs was determined in a chromium[51] release assay. All target cells are HLA-A2[+]. The allo–HLA-A2 CTL clone lyses all target cells, the HA-1 CTL clones lyse only HA-1^{+} target cells, and the H-Y CTL clone lyses only H-Y^{+} target cells. X-axis represents the mean percentage specific lysis (2 measurements per condition); y-axis, CTL clones each in 2 different effector to target ratios. EBV LCL indicates Epstein-Barr virus/lymphoid cell line.

HA-1 CTLs eradicate human 3D microtumors in vitro

To assess the efficacy and mHag specificity of particularly HA-1 CTLs against human microtumors in vitro, we developed an in vitro model allowing real-time assessment of immunotherapeutic effects on individual human 3D microtumors (L.H. and E.G., manuscript in preparation). Tumor cell agglomerates were embedded in a collagen scaffold resulting in progressively growing tumors. Microtumors showed a multilayer morphology on days 3 (data not shown) and 7 (Figure 2E-H) mimicking clinical cancers of the same entities as the tumors from which the tumor cell lines were derived (Table S1), both histopathologically (Figure 2A-D) and immunohistochemically (L.H., E.G., manuscript in preparation). We applied these microtumors to investigate mHag CTL-mediated tumor clearance, CTL-tumor infiltration, and cytokine release within one model. Microtumors were generated on day 0 and medium alone, HA-1, or H-Y CTLs were added on day 1. CTLs required 2 to 3 days to reach the microtumors as determined by light microscopy. On day 7, all HLA-A2[+] microtumors were destroyed by the allo–HLA-A2 CTL clone 1E2 (data not shown). All 3 HA-1 CTLs clones 1.7, 2.12, and 3HA15 eliminated at an effector to target ratio of 15:1 the HA-1^{+} microtumors BB65-RCC (Figure 2E) and MDA-MB 231 (Figure 2F), while leaving the HA-1^{−} microtumors 518A2 (Figure 2G) and MCF-7 (Figure 2H) intact. The H-Y CTL clone 21–17 destroyed only the H-Y[+] microtumors BB65-RCC (Figure 2E) and 518A2 (Figure 2G) without affecting growth of the H-Y[−] microtumors MDA-MB 231 (Figure 2F) and MCF-7 (Figure 2H). Immunohistochemistry on day 3 revealed that all HA-1 and H-Y CTL clones infiltrate all microtumors. However, the extent of microtumor infiltration by mHag CTLs was dependent on the expression of the relevant mHag by the microtumors (Figure 3A,B; Figure S3). Longitudinal assessment of the tumor size on days 3 and 7 revealed that all mHag CTL clones inhibited tumor growth in a mHag-specific and CTL dose-dependent manner (Figure 3C). Prolongation of the observation period from 7 to 14 days in the mHag specifically treated groups showed no progression of microtumors (Figure S4A). Antitumor effects of HA-1 and H-Y CTLs were associated with mHag-specific release of interferon-γ (IFN-γ), which was maximal on day 3 and subsequently declined (Figure 3D). These results
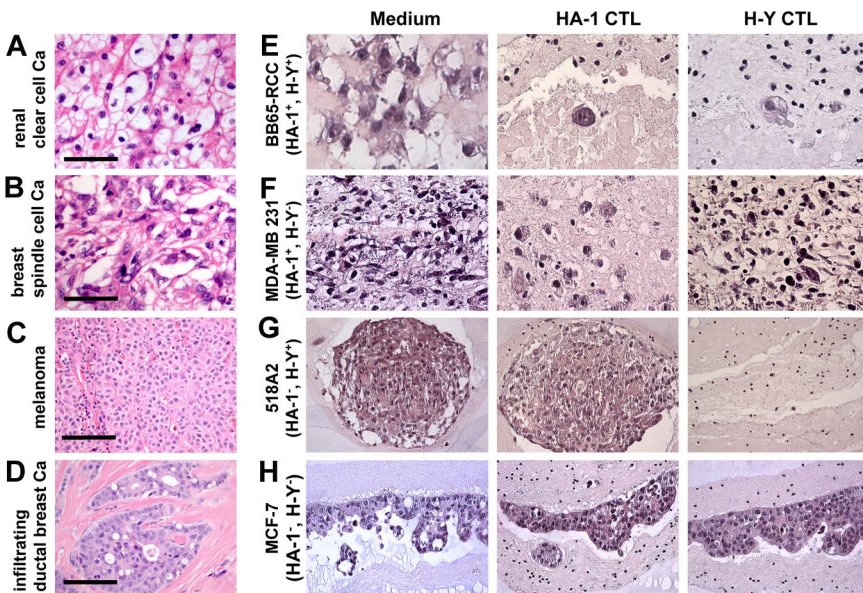
between the tumor cell lines, whereas the expression of cell adherence molecules was comparable (Figure S1B). mHag-specific cytotoxicity of the previously established HA-1 CTL clones 1.7, 2.12, and 3HA15 and the H-Y CTL clone 21–17 was tested in a standard 4-hour ^{51}Cr-release assay. The HA-1 CTL clones lysed only HA-1^{+} target cells, including the RCC cell line BB65-RCC and the breast cancer cell line MDA-MB-231 (Figure 1A-C). The H-Y CTL clone lysed only H-Y^{+} target cells, including the RCC cell line BB65-RCC and the melanoma cell line 518A2 (Figure 1A,B,E). The avidity of the different HA-1 CTLs clones for their target cells was comparable (Figure S2A). All HA-1 CTL clones used in this study displayed a marker profile consistent with a terminally differentiated effector memory T-cell phenotype (CD3^{+}, CD8^{+}, CD45RA^{−}, CD62L^{−}, CD27^{−}, CD28^{−}) (Figure S2B).

Figure 2. HA-1 CTLs eradicate 3D microtumors mimicking primary tumors. H&E stainings reveal that microtumors (E-H medium controls) closely resemble the histologies of the corresponding primary tumors (A-D). BB65-RCC microtumors (E) show clear cells similar to a primary intermediately differentiated renal cell carcinoma (A). MDA-MB 231 microtumors (F) contain spindle-formed cells without orientation similar to a primary spindle cell carcinoma of the breast (B). 518A2 microtumors (G) show sheets of cells similar to a primary melanoma (C). MCF-7 microtumors (H) show acinus-like structures similar to a primary intraductal carcinoma (D). (E-H) HA-1 and H-Y CTLs destroy microtumors in a strictly mHag-specific manner, resulting in strongly reduced cellularity and cell debris. Bars in top 2 rows represent 100 μm; in bottom 2 rows, 50 μm.
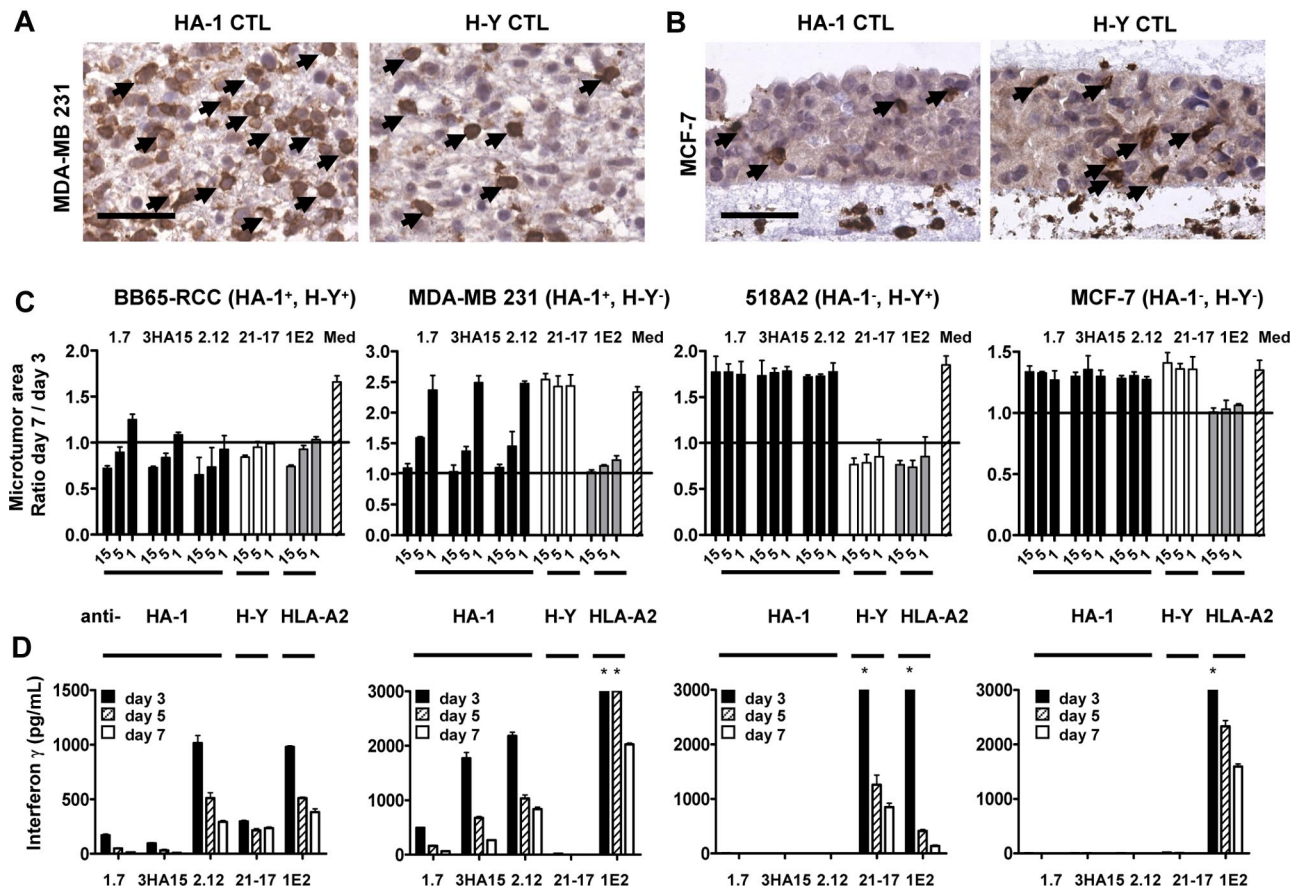
Figure 3. HA-1 CTLs infiltrate 3D microtumors, inhibit tumor growth, and release IFN-γ. (A-B) CD8 staining of MDA-MB 231 (A) and MCF-7 (B) microtumors after 3 days of coincubation with HA-1 or H-Y CTLs. Arrowheads indicate CD8+ CTLs; bar represents 50 μm. (C) Microtumor growth inhibition after addition of the anti–HA-1, H-Y, or HLA-A2 CTLs. X-axis represents CTL clones each in 3 different effector-target ratios (15:1, 5:1, 1:1) or medium; y-axis, ratio between the microtumor areas in photographs of day 7 and day 3. Bars correspond to means plus or minus SEM (data are pooled from 3 independent experiments resulting in median 3 [range, 2-8] microtumors per condition). (D) IFN-γ in the supernatant of microtumors after addition of anti–HA-1, H-Y CTL, and HLA-A2 CTLs in an effector to target ratio of 15:1. X-axis represents days 3, 5, and 7 after addition of different CTL clones; y-axis, IFN-γ in the supernatant. Bars correspond to means plus or minus SEM (4 measurements per sample). Asterisk indicates off-scale measurement.

demonstrate that HA-1 CTLs can eradicate human solid tumors in a highly mHag-specific manner and that H-Y CTLs are equally effective.

In vivo distribution of HA-1 CTLs

Due to their restricted tissue expression, only tumor mHags (such as HA-1) are suitable as targets for mHag-specific immunotherapy of solid tumors after allogeneic SCT. To investigate whether CTLs directed at a single tumor mHag HA-1 are capable of eradicating solid tumors in vivo, we designed translational animal models. In these models, human solid tumors were engrafted in immunodeficient nonobese diabetic/severe combined immunodeficient (NOD/scid) mice and subsequently treated with human mHag CTLs. Based on its aggressive localized and metastatic growth,[21] we selected the HA-1+/H-Y− breast cancer cell line MDA-MB 231 as tumor target in our in vivo experiments. Subcutaneous macrotumors were established in NOD/scid mice by subcutaneous injection of 5×10^6 MDA-MB 231 cells, which induced progressively growing tumors of 8- to 10-mm diameter on day 30 in all mice (data not shown). Aiming to treat human subcutaneous macrotumors in NOD/scid mice, we determined survival, in vivo distribution, and tumor infiltration of HA-1 CTLs. We selected for comparative adoptive CTL transfer experiments the best expandable HA-1 CTL clone 1.7 used in this study (data not shown). Mice with a tumor diameter of 6 to 8 mm received 30×10^6 HA-1 CTLs

intravenously. Tracking of adoptively transferred HA-1 CTLs on days 1, 3, 7, 14, and 21 after CTL administration showed systemic distribution of human CTLs into lung, liver, spleen, bone marrow, and peripheral blood (% infiltrations of the analyzed organs by HA-1 CTLs are depicted in Figure 4A; absolute numbers of HA-1 CTLs in the analyzed organs are depicted in Figure S5). On day 1 after CTL transfer, CTL infiltration was highest in the lungs, whereas all other organs showed infiltration at lower and comparable levels. HA-1 CTLs redistributed from the lungs on day 1 to the bone marrow on day 3 (Figure S5). HA-1 CTL infiltration of the various organs persisted for up to 14 days after CTL administration, most pronounced in the bone marrow. No HA-1 CTLs were found in the peripheral blood beyond day 3. At none of the time points analyzed were substantial levels of HA-1 CTLs detected in subcutaneous macrotumors (Figure 4A; Figure S5). Thus, we did not continue to perform experiments determining the in vivo efficacy of HA-1 CTLs against subcutaneous macrotumors.

HA-1 CTLs hardly infiltrate HA-1+ human subcutaneous macrotumors ex vivo

The absence of HA-1 CTLs in macrotumors led us to question HA-1 expression in subcutaneous macrotumors in vivo. Single-cell suspensions of MDA-MB 231 macrotumors freshly explanted from untreated mice (ie, without previous HA-1 CTL infusion) were,
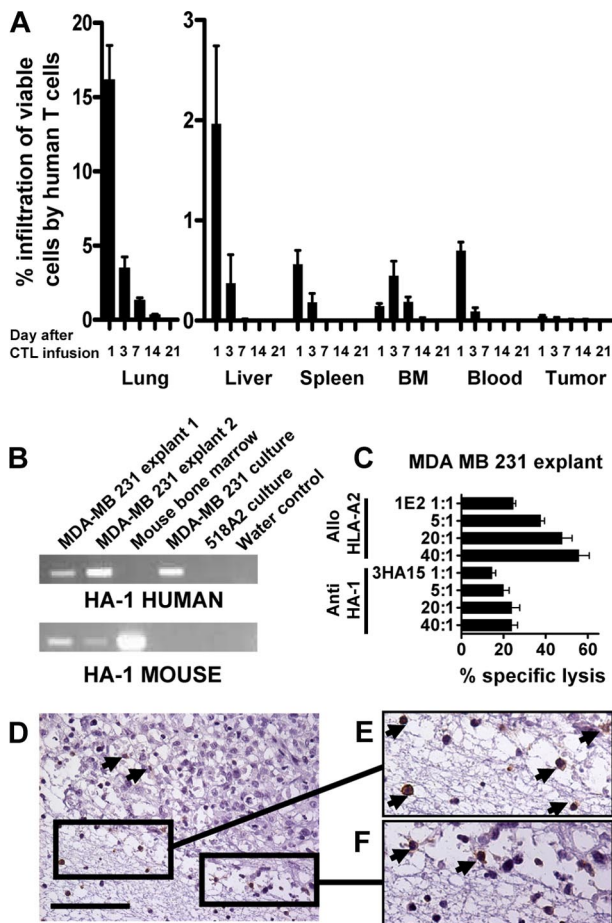
Figure 4. In vivo distribution of HA-1 CTLs and ex vivo analysis of subcutaneous macrotumors. (A) NOD/scid mice with subcutaneous MDA-MB 231 macrotumors were treated with a single dose of 30×10^6 HA-1 CTLs (clone 1.7) intravenously. HA-1 CTLs were quantified by flow cytometry in lung, liver, spleen, bone marrow, peripheral blood, and the solid tumor at 1, 3, 7, 14, or 21 days after CTL transfer. Depicted is the percentage of viable human CTLs in relation to all measured viable cells in the individual tissues. Bars correspond to means plus or minus SEM (4 mice per measurement time point). (B) HA-1 mRNA expression in single-cell suspensions of MDA-MB 231 macrotumors freshly explanted from 2 individual untreated (ie, without HA-1 CTL infusion) NOD/scid mice, mouse bone marrow, and cultured MDA-MB 231 and 518A2 cells determined with human (top row) and mouse (bottom row) HA-1–specific primers. Weak mouse HA-1 mRNA signals in the explanted tumor samples indicate contamination with mouse hematopoietic cells. (C) Single-cell suspensions of MDA-MB 231 macrotumors freshly explanted from 3 individual untreated NOD/scid mice were lysed by allo–HLA-A2 and HA-1 CTLs. X-axis represents percentage of specific lysis (means plus or minus SEM); y-axis, CTL clones in 4 different effector-target ratios. (D-F) Biopsies of MDA-MB 231 subcutaneous macrotumors explanted from untreated NOD/scid mice were embedded in collagen type I matrix and coincubated with the HA-1 CTL clones 1.7, 2.12, and 3HA15 for 3 days. Shown is a representative example of a human CD8 staining. HA-1 CTLs are present only in the surrounding collagen type I matrix and the tumor border. Arrowheads indicate CD8$^+$ CTLs; bar represents 100 μm.

however, positive for HA-1 mRNA (Figure 4B) and were recognized by allo–HLA-A2 and HA-1 CTLs in a 4-hour ^{51}Cr-release assay (Figure 4C). Moreover, growth of microtumors generated from explanted tumor cells was equally well inhibited by HA-1 CTLs as microtumors generated from MDA-MB 231 cells without in vivo passage (Figure S4B). Thus, MDA-MB 231 tumor cells maintain functional HLA-A2/HA-1 expression upon in vivo growth. Next, we determined whether absence of tumor infiltration by CTLs was related to the characteristic of one individual HA-1 CTL clone. Thus, we embedded 3-mm punch biopsies of MDA-MB 231 macrotumors explanted from untreated mice in collagen type I matrix and coincubated these biopsies with 10^6 cells of the HA-1

CTL clones 1.7, 2.12, and 3HA15. CD8 staining on parallel sections on day 3 showed abundant presence of all HA-1 CTL clones in the collagen matrix and on the tumor border, but only very few HA-1 CTLs within the tumor (Figure 4D-F). Thus, HA-1 CTLs hardly infiltrate human subcutaneous macrotumors, despite in vivo maintenance of HA-1 expression.

HA-1 CTLs prevent and inhibit the progression of human lung metastases in vivo

Subsequently, we investigated whether the direct HA-1 CTL–human tumor cell in vivo interaction is effective in preventing pulmonary metastasis. Intravenous injection of HA-1$^+$/H-Y$^-$ MDA-MB 231 tumor cells in the lateral tail vein on day 0 resulted in median 37 (range, 4-80) and 159 (range, 111-399) pleural tumor nodules on the intact lungs after 40 and 50 days (representative examples are depicted in Figure 5A), respectively. Cytokeratin staining on parallel sections revealed microtumors in the pulmonary interstitium of which some were subpleurally localized (Figure 5B). Quantification of the microtumors revealed median 13 (range, 2.3-40.1) and 25 (range, 19.2-48.1) microtumors per section after 40 and 50 days, respectively. No metastases in other organs (liver, spleen, bone marrow, kidneys) were found (data not shown). Three days after intravenous inoculation of MDA-MB 231 tumor cells, when disseminated tumor cells were already detectable (Figure 5E), a single dose of 30×10^6 HA-1 CTLs, H-Y CTLs, or PBS as control was administered intravenously. HA-1 CTLs and H-Y CTLs showed comparable kinetics in the peripheral blood and were undetectable after 3 days upon CTL administration (Figure S6). Mice having received the control H-Y CTLs or PBS showed on days 40 and 50 no significant difference in the number of pleural tumor nodules ($P = .468$, $P = .754$) or intrapulmonal microtumors ($P = .386$, $P = .602$), which excluded unspecific effects due to the procedure of CTL infusion (Figure 5C,D). In contrast, mice injected with the HA-1 CTL clone showed pleural tumor nodules in none of the mice on day 40 (difference in number of pleural tumor nodules compared with the PBS- and H-Y CTL–treated groups: $P = .014$ and $P = .014$, respectively) or in only 1 of 6 mice on day 50 ($P = .004$ and $P = .007$, respectively) (Figure 5C). Intrapulmonal microtumors after treatment with HA-1 CTLs were detectable in 3 of 4 mice on day 40 (difference in number of intrapulmonal microtumors compared with the PBS- and H-Y CTL–treated groups: $P = .021$ and $P = .021$, respectively) or in 2 of 6 mice on day 50 ($P = .005$ and $P = .009$, respectively; Figure 5D). Thus, HA-1 CTLs eradicate disseminated tumor cells and, thereby, prevent human metastases in NOD/scid mice. Subsequently, we tested the antitumor efficacy of HA-1 CTLs against fully established pulmonary metastases. NOD/scid mice engrafted with MDA-MB 231 tumor cells intravenously were injected with a single dose of 30×10^6 HA-1 CTLs or H-Y CTLs or PBS as control intravenously on day 40. On day 50, mice were killed. Immunohistochemistry showed infiltration of pulmonary metastases by HA-1 CTLs (Figure 5F). Quantification of pulmonary tumors revealed no significant difference in the number of pleural tumor nodules ($P = .522$) or intrapulmonal microtumors ($P = .631$) in the control groups (PBS and H-Y CTLs). In contrast, mice injected with the HA-1 CTL clone showed significantly less pleural (difference in number of tumor nodules compared with the PBS- and H-Y CTL–treated groups: $P = .005$ and $P = .004$, respectively) (Figure 5C) and intrapulmonal tumor nodules ($P = .005$ and $P = .009$, respectively; Figure 5D). Thus, HA-1 CTLs inhibit

Figure 5. HA-1 CTLs prevent and inhibit the progression of pulmonary metastases. NOD/scid mice received human HA-1⁺/H-Y⁻ MDA-MB 231 breast cancer cells intravenously on day 0 and were treated with PBS or 30×10^6 HA-1 or H-Y CTLs intravenously. (A,B) Depicted are representative examples of lungs of mice that had been treated with PBS (left), the HA-1 CTL clone 1.7 (middle), and the H-Y CTL clone 21–17 (right) on day 3 and killed on day 50. Larger pleural tumor nodules are macroscopically visible (A). Cytokeratin staining shows microtumors in the pulmonary interstitium of which some were subpleurally localized; bar represents 500 μm (B). Arrows indicate tumors. (C,D) Quantification of pulmonary tumors of mice that had been treated on day 3 and killed on day 40 (left graphs; 4 mice per group, 5×10^5 tumor cells per mouse) or on day 50 (middle graphs, 5-6 mice per group, 7.5×10^5 tumor cells per mouse); quantification of pulmonary tumors of mice that had been treated on day 40 and killed on day 50 (right graphs, 6 mice per group, 7.5×10^5 tumor cells per mouse). X-axis represents treatment with PBS, HA-1, or H-Y CTLs; y-axis, number of pleural tumor nodules visible on the intact lungs (C) or number of intrapulmonal microtumors per parallel section (D). Numbers of lung tumors were pairwise compared in different groups of mice by Mann-Whitney U test. n.s. indicates not significant. (E) Cytokeratin staining of single tumor cells in the lungs of mice 3 days after intravenous administration of MDA-MB 231 tumor cells; bar represents 50 μm. (F) CD8 staining of a pulmonary metastasis of mice that had been treated on day 40 with HA-1 CTLs and killed on day 50. Arrows indicate CD8⁺ CTLs; bar represents 50 μm.
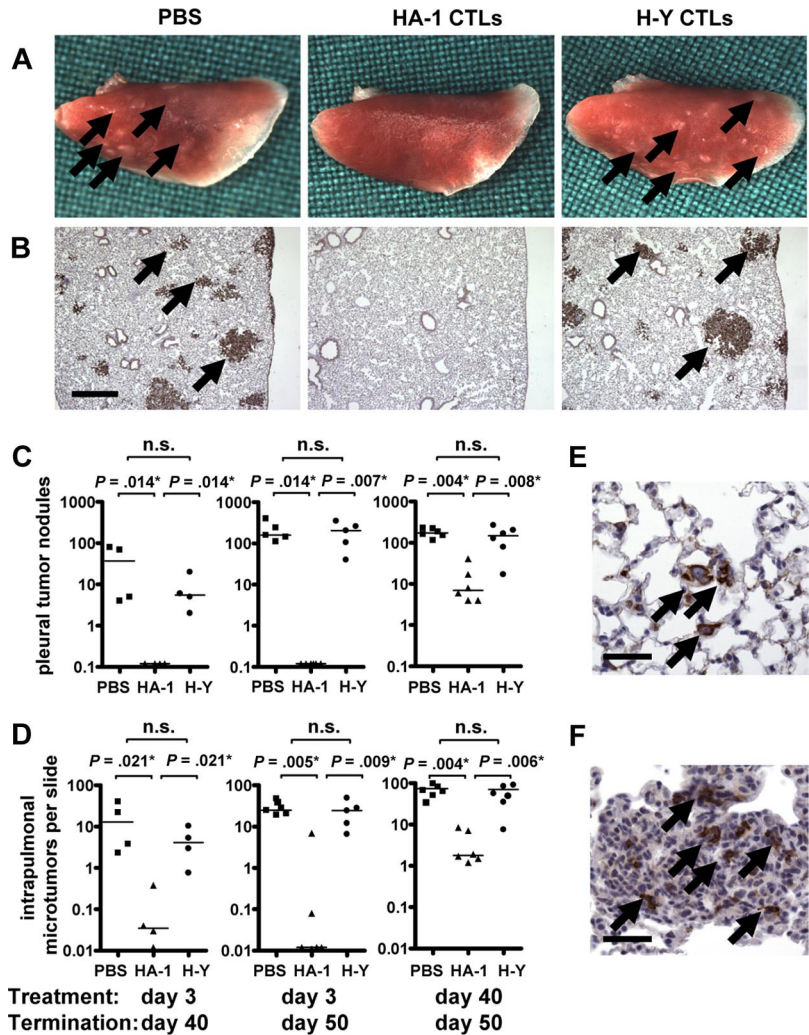
the progression of fully established human cancer metastases in NOD/scid mice.

Discussion

Our study is the first to show the potency and mHag specificity of human mHag HA-1 CTLs to destroy human 3D microtumors that closely resemble clinical micrometastases and avascular tumor stages. Although mHag HA-1 expression on single tumor cells has been described,[12,13,22] its clinically relevant functional expression on 3D tumors was as yet unknown. Tumor eradication by HA-1 CTLs points toward crucial differences in the functional expression of the mHag HA-1 on solid tumors compared with tumor-associated antigens (TAAs), which are commonly used as targets for cancer immunotherapy. Although 3D tumor growth results in loss of TAA presentation[23,24] and in "multicellular apoptosis resistance"[25,26] within 24 hours, the functional mHag HA-1 expression and tumor susceptibility to mHag CTL lysis were not hampered by the 3D tumor growth in our study. Interestingly, complete microtumor eradication has not been shown for human TAA-specific CTLs, to the best of our knowledge. A possible explanation might be the frequently lacking TAA expression in a considerable proportion of cancer cells in clinical tumors, as shown for melanocyte differentiation (eg, MelanA/MART-1 or gp100)[27]

and for cancer testis antigens (eg, MAGE-1 or NY-ESO-1).[28,29] In addition, experimental 518A2 melanomas used in our study were only heterogeneously positive for MelanA (data not shown). The complete eradication of microtumors by HA-1 CTLs provides a first indication that HA-1 is expressed on the vast majority of tumor cells in our model. Nevertheless, it needs to be considered that primary tumors may have a more complex hierarchy of cancer stem cells and progeny than reflected by tumor cell lines in our model. Thus, further studies using HA-1–specific antibodies or probes for mRNA in situ hybridization are required to exactly determine the homogeneity of HA-1 expression, particularly in clinical tumors. Overall, the capability of HA-1 CTLs to infiltrate microtumors, to inhibit tumor growth, and, ultimately, to eradicate human microtumors in a highly mHag-specific manner qualifies HA-1 as powerful allogeneic target on solid tumors.

However, after HLA-matched allogeneic SCT, the tumor mHag HA-1 is only one of many mismatched mHags driving the GVH response. Accordingly, also CTLs directed against the GVHD target antigen H-Y were highly effective in eradicating human solid tumors in our study in vitro. In fact, both mHag CTLs against tumor mHags (HA-1) and against ubiquitously expressed mHags (HA-3 and HA-8) are detectable in solid tumor patients responding to allogeneic SCT.[22] The individual contribution of CTLs against tumor mHags and CTLs against ubiquitously expressed mHags to the GVT effect is unknown. However, the high efficacy of HA-1
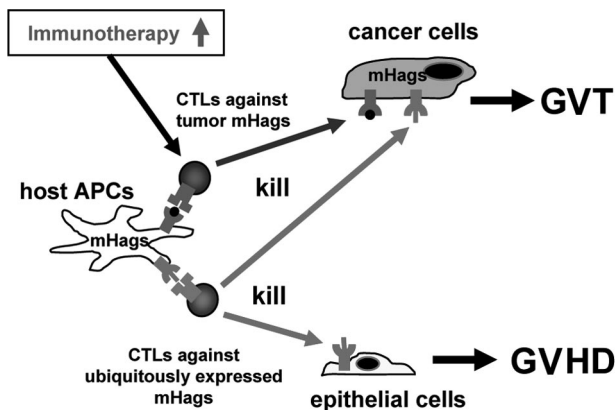
Figure 6. Targeting solely mismatched tumor mHags boosts the GVT effect. HLA-matched patients and donors remain mismatched for multiple mHags. According to our working hypothesis, host-derived antigen presenting cells (APCs) persisting after allogeneic SCT induce an antihost response of donor T cells. Based on the mHag tissue distribution, the antihost response is dissected into a branch mediating only GVT effects and a branch mediating both GVT effects and GVHD. Our findings indicate that immunotherapy targeting only mismatched tumor mHags is sufficient to boost the GVT effect.

CTLs in our study in vitro indicates that solely targeting tumor mHags might be sufficient to boost the anti–solid tumor response in vivo (Figure 6).

Accordingly, adoptive transfer of a single dose of HA-1 CTLs was highly effective in eradicating disseminated tumor cells and, thereby, preventing pulmonary breast cancer metastases in our study in vivo. Although eradication of murine tumors by targeting a ubiquitously expressed murine mHag was recently demonstrated by Perreault and coworkers (Meunier et al[30]), we here show for the first time the in vivo antitumor efficacy of CTLs directed against a human tumor-restricted and, thus, clinically relevant mHag. Several factors might have contributed to the high in vivo efficacy of HA-1 CTLs. First, adoptively transferred CTLs temporarily accumulated in the lungs on day 1. Thus, administered CTLs passively encounter lung metastases via the pulmonary circulation. Of note, the systemic distribution of HA-1 CTLs observed in the macrotumor model indicates that HA-1 CTLs have the potential to eliminate solid tumor cells at all possible sites of metastases in all organs. Second, the high CTL to tumor cell ratio ($> 40:1$) has likely contributed to the anti–solid tumor efficacy of HA-1 CTLs. This assumption is supported by the CTL dose-dependent long-term efficacy of mHag CTLs against microtumors in vitro and our previous observation that HA-1 CTLs were effective only against minimal leukemic disease in NOD/scid mice, whereas not against overt leukemia.[20] Finally, the direct contact of administered CTLs with the disseminated tumor cells without the need of tumor infiltration may have facilitated the antitumor efficacy of HA-1 CTLs in this model. However, HA-1 CTLs also inhibited the progression of pulmonary metastases fully established as 3D tumor structures. This finding is particularly relevant in cases in which complete remissions cannot be achieved by conventional treatments before HA-1–specific immunotherapy. Overall, our in vivo data demonstrate that HA-1 CTLs are therapeutically highly effective against solid tumors in minimal disease.

In contrast, subcutaneous macrotumors represented a limitation in our NOD/scid mouse tumor model, as in this setting hardly any tumor-infiltrating HA-1 CTLs could be detected. This finding reflects conflicting data on tumor infiltration by TAA CTLs upon adoptive transfer in humans. Despite indications for infiltration by TAA CTLs found in some metastatic melanoma lesions of few evaluated patients,[31-33] most metastases seemed to be spared by TAA CTLs. The reasons for low tumor infiltration by human CTLs specific for single tumor epitopes are poorly understood. In our in vivo subcutaneous macrotumor model, the systemic distribution of transferred CTLs suggests that HA-1 CTLs can reach the circulation of the well-vascularized MDA-MB 231 tumors (data not shown). Potential difficulties for CTLs to home to tumors or to cross the xenogeneic tumor endothelium cannot be excluded by our experiments. However, we have ruled out a loss of functional HLA-A2/HA-1 target antigen expression in vivo. The fact that all 3 tested HA-1 CTL clones were hardly detectable in tumor biopsies upon in vitro coincubation makes an individual characteristic of one particular CTL clone unlikely as a reason for low macrotumor infiltration. The absence of human HA-1 cross-presentation by mouse stromal cells in subcutaneous macrotumors may lead to insufficient stimulation of CTL migration.[34] In addition, CTL deletion by, for example, intratumoral nutrition deprivation or "tumor counterattack"[9] needs to be considered. However, our finding that in vitro microtumors and pulmonary metastases were—in contrast to subcutaneous macrotumors—considerably infiltrated by HA-1 CTLs might also point toward differences in the composition of the various MDA-MB 231 tumors. In fact, the compactness of the tumor histology increased from in vitro microtumors over pulmonary metastases to subcutaneous macrotumors (Figure S7A). Moreover, the higher compactness of the larger (8 mm at explant) subcutaneous macrotumors compared with the smaller (< 1 mm) pulmonary metastases was associated with a much higher content of connective tissue (ie, desmoplasia) in these tumors in vivo (Figure S7B,C). Thus, the tumor architecture might, in analogy with applying antibodies[35] and chemical antitumor agents[36] and as indicated by previous reports,[37-39] represent a physical barrier for CTL infiltration. The in vitro and in vivo models presented in this study might help to further verify this hypothesis and to identify specific molecules in the extracellular matrix of tumors accessible for therapeutic intervention to reduce this CTL barrier. Since desmoplasia in humans correlates with the progression of solid tumors,[40] our data suggest that there are at least 2 interrelated factors associated with a high tumor load hampering the success of allogeneic immunotherapy, namely the unfavorable in vivo effector to target cell ratio and the tumor composition. These data may partially explain the experience after allogeneic SCT for leukemia[7,41] and solid tumor[42] treatment, that alloimmunotherapeutic effects are generally most successful in minimal residual disease. Thus, optimally, tumor reduction by, for example, surgery, chemotherapy, or radiotherapy should precede a consolidation with allogeneic SCT combined with tumor mHag-specific immunotherapy.

Evidently, T-cell depletion with subsequent infusion of only tumor mHag-specific CTLs is the safest form of exploiting tumor mHag mismatches between donor and patient. However, murine studies suggest that GVHD provides an optimal proinflammatory environment for the efficacy of CTLs directed against tumor-restricted antigens.[43] Of course, questions regarding the interplay between GVHD and GVT effects cannot be addressed in our in vivo models, because of the absence of human GVHD target antigens in NOD/scid mice. Ongoing and future clinical studies will show whether tumor mHag CTLs are most effective during mild and manageable GVHD, thus favoring non–T cell–depleted allogeneic SCT or donor lymphocyte infusions as platform for tumor mHag-specific immunotherapy of solid tumors.[7]

Conclusions

We have shown the first proof of concept that tumor mHag CTLs can induce strong effects against metastatic cancer in vivo. Thus, mismatched mHags with hematopoiesis- and solid tumor–restricted expression are excellent tools to boost the alloimmune response against solid tumors after HLA-matched allogeneic SCT. These findings pave the way toward alloimmunotherapy protocols for metastatic cancer that do not risk severe GVHD and that overcome—due to the allo-ness of the mHag target molecules—the major limitation of current immunotherapies in the autologous setting, namely self-tolerance. A novel approach for enhancing the alloimmune response against tumor mHags is mHag peptide vaccination. Tumor mHag CTLs "naturally" arising after HLA-matched allogeneic SCT may be boosted by repetitive administration of the patient's mHag peptides—an approach we are currently testing in a first phase 1/2 study for patients with renal cell carcinoma.

Acknowledgments

Authorship

Contribution: L.H. conducted all and performed most of the experiments, prepared the figures, and drafted the paper; M.V. supported the animal experiments and performed all histologies and immunohistochemistries; A.B. helped in performing the microtumor experiments; Z.A. maintained the cell cultures and helped with the T-cell assays; T.K. supervised the project and edited the paper; and E.G. initiated and supervised the project and edited the paper.

Conflict-of-interest disclosure: The authors declare no competing financial interests.

Correspondence: Lothar Hambach, Department of Immunohematology and Blood Transfusion, E3Q, Leiden University Medical Center, PO-Box 9600, 2300 RC Leiden, The Netherlands; e-mail: l.w.h.hambach@lumc.nl.

References

1. Eibl B, Schwaighofer H, Nachbaur D, et al. Evidence for a graft-versus-tumor effect in a patient treated with marrow ablative chemotherapy and allogeneic bone marrow transplantation for breast cancer. Blood. 1996;88:1501-1508.

2. Ueno N, Rondon G, Mirza N, et al. Allogeneic peripheral-blood progenitor-cell transplantation for poor-risk patients with metastatic breast cancer. J Clin Oncol. 1998;16:986-993.

3. Childs R, Chernoff A, Contentin N, et al. Regression of metastatic renal-cell carcinoma after nonmyeloablative allogeneic peripheral-blood stem-cell transplantation. N Engl J Med. 2000;343:750-758.

4. Bregni M, Dodero A, Peccatori J, et al. Nonmyeloablative conditioning followed by hematopoietic cell allografting and donor lymphocyte infusions for patients with metastatic renal and breast cancer. Blood. 2002;99:4234-4236.

5. Bishop M, Fowler D, Marchigiani D, et al. Allogeneic lymphocytes induce tumor regression of advanced metastatic breast cancer. J Clin Oncol. 2004;22:3886-3892.

6. Carella AM, Beltrami G, Corsetti MT, et al. Reduced intensity conditioning for allograft after cytoreductive autograft in metastatic breast cancer. Lancet. 2005;366:318-320.

7. Hambach L, Goulmy E. Immunotherapy of cancer through targeting of minor histocompatibility antigens. Curr Opin Immunol. 2005;17:202-210.

8. Goulmy E. Human minor histocompatibility antigens. Curr Opin Immunol. 1996;8:75-81.

9. Mapara M, Sykes K. Tolerance and cancer: mechanisms of tumor evasion and strategies for breaking tolerance. J Clin Oncol. 2004;22:1136-1151.

10. de Bueger M, Bakker A, van Rood J, van der Woude F, Goulmy E. Tissue distribution of human minor histocompatibility antigens: ubiquitous versus restricted tissue distribution indicated heterogenity among human cytotoxic T lymphocyte-defined non-MHC antigens. J Immunol. 1992; 149:1788-1794.

11. Dickinson A, Wang X, Sviland L, et al. In situ dissection of the graft-versus-host activities of cytotoxic T cells specific for minor histocompatibility antigens. Nat Med. 2002;8:410-414.

12. Klein C, Wilke M, Pool J, et al. The hematopoietic system-specific minor histocompatibility antigen HA-1 shows aberrant expression in epithelial cancer cells. J Exp Med. 2002;196:359-368.

13. Fujii N, Hiraki A, Ikeda K, et al. Expression of minor histocompatibility antigen, HA-1, in solid tumor cells. Transplantation. 2002;73:1137-1141.

14. Akatsuka Y, Nishida T, Kondo E, et al. Identification of a polymorphic gene, BCL2A1, encoding two novel hematopoietic lineage-specific minor histocompatibility antigens. J Exp Med. 2003;197: 1489-1500.

15. Spierings E, Drabbels J, Hendriks M, et al. A uniform genomic minor histocompatibility antigen typing methodology and database designed to facilitate clinical applications. PLoS ONE (http://www.plosone.org/). 2006;1:e42.

16. Mutis T, Verdijk R, Schrama E, et al. Feasibility of immunotherapy of relapsed leukemia with ex vivo-generated cytotoxic T lymphocytes specific for hematopoietic system-restricted minor histocompatibility antigens. Blood. 1999;93:2336-2341.

17. Spierings E, Vermeulen C, Vogt M, et al. Identification of HLA class II-restricted H-Y specific T helper epitope evoking CD4+ T-helper cells in H-Y-mismatched transplantation. Lancet. 2003; 362:610-615.

18. Wei W, Miller B, Gutierrez R. Inhibition of tumor growth by peptide specific cytotoxic T lymphocytes in a three-dimensional collagen matrix. J Immunol Methods. 1997;200:47-54.

19. Nijmeijer B, Willemze R, Falkenburg J. An animal model for human cellular immunotherapy: specific eradication of human acute lymphoblastic leukemia by cytotoxic T lymphocytes. Blood. 2002;100:654-660.

20. Hambach L, Nijmeijer B, Aghai Z, et al. Human cytotoxic T lymphocytes specific for a single minor histocompatibility antigen HA-1 are effective against human lymphoblastic leukaemia in NOD/scid mice. Leukemia. 2006;20:371-374.

21. Price JE, Polyzos A, Zhang RD, Daniels LM. Tumorigenicity and metastasis of human breast carcinoma cell lines in nude mice. Cancer Res. 1990;50:717-721.

22. Tykodi S, Warren E, Thompson J, et al. Allogeneic hematopoietic cell transplantation for metastatic renal cell carcinoma after nonmyeloablative conditioning: toxicity, clinical response, and immunological response to minor histocompatibility antigens. Clin Cancer Res. 2004;10:7799-7811.

23. Dangles-Marie V, Richon S, El Behi M, et al. A three-dimensional tumor cell defect in activating autologous CTLs is associated with inefficient antigen presentation correlated with heat shock protein-70 down regulation. Cancer Res. 2003; 63:3682-3687.

24. Feder-Mengus C, Ghosh S, Weber WP, et al. Multiple mechanisms underlie defective recognition of melanoma cells cultured in three-dimensional architectures by antigen-specific cytotoxic T lymphocytes. Br J Cancer. 2007;96: 1072-1082.

25. Sutherland RM. Cell and environment interactions in tumor microregions: the multicell spheroid model. Science. 1988;240:177-184.

26. Desoize B, Jardillier J. Multicellular resistance: a paradigm for clinical resistance? Crit Rev Oncol Hematol. 2000;36:193-207.

27. de Vries TJ, Smeets M, de Graaf R, et al. Expression of gp100, MART-1, tyrosinase, and S100 in paraffin-embedded primary melanomas and locoregional, lymph node, and visceral metastases: implications for diagnosis and immunotherapy: a study conducted by the EORTC Melanoma Cooperative Group. J Pathol. 2001;193:13-20.

28. Jungbluth AA, Stockert E, Chen YT, et al. Monoclonal antibody MA454 reveals a heterogeneous expression pattern of MAGE-1 antigen in

formalin-fixed paraffin embedded lung tumours. Br J Cancer. 2000;83:493-497.

29. Jungbluth AA, Chen YT, Stockert E, et al. Immunohistochemical analysis of NY-ESO-1 antigen expression in normal and malignant human tissues. Int J Cancer. 2001;92:856-860.

30. Meunier MC, Delisle JS, Bergeron J, et al. T cells targeted against a single minor histocompatibility antigen can cure solid tumors. Nat Med. 2005;11:1222-1229.

31. Meidenbauer N, Marienhagen J, Laumer M, et al. Survival and tumor localization of adoptively transferred Melan-A specific T cells in melanoma patients. J Immunol. 2003;170:2161-2169.

32. Vignard V, Lemercier B, Lim A, et al. Adoptive transfer of tumor-reactive Melan-A-specific CTL clones in melanoma patients is followed by increased frequencies of additional Melan-A-specific T cells. J Immunol. 2005;175:4797-4805.

33. Yee C, Thompson JA, Byrd D, et al. Adoptive T cell therapy using antigen-specific CD8+ T cell clones for the treatment of patients with metastatic melanoma: in vivo persistence, migration,

and antitumor effect of transferred T cells. Proc Natl Acad Sci U S A. 2002;99:16168-16173.

34. Zhang B, Bowerman NA, Salama JK, et al. Induced sensitization of tumor stroma leads to eradication of established cancer by T cells. J Exp Med. 2007;204:49-55.

35. Netti PA, Berk DA, Swartz MA, Grodzinsky AJ, Jain RK. Role of extracellular matrix assembly in interstitial transport in solid tumors. Cancer Res. 2000;60:2497-2503.

36. Minchinton AI, Tannock IF. Drug penetration in solid tumours. Nat Rev Cancer. 2006;6:583-592.

37. Yang Q, Goding S, Hagenaars M, et al. Morphological appearance, content of extracellular matrix and vascular density of lung metastases predicts permissiveness to infiltration by adoptively transferred natural killer and T cells. Cancer Immunol Immunother. 2006;55:699-707.

38. Kuppen PJ, van der Eb MM, Jonges LE, et al. Tumor structure and extracellular matrix as a possible barrier for therapeutic approaches using immune cells or adenoviruses in colorectal cancer. Histochem Cell Biol. 2001;115:67-72.

39. Singh S, Ross SR, Acena M, Rowley DA, Schreiber H. Stroma is critical for preventing or permitting immunological destruction of antigenic cancer cells. J Exp Med. 1992;175:139-146.

40. Kääriäinen E, Nummela P, Soikkeli J, et al. Switch to an invasive growth phase in melanoma is associated with tenascin-C, fibronectin, and procollagen-I forming specific channel structures for invasion. J Pathol. 2006;210:181-191.

41. Barrett J. Allogeneic stem cell transplantation for chronic myeloid leukemia. Semin Hematol. 2003;40:59-71.

42. Carella AM, Bregni M. Current role of allogeneic stem cell transplantation in breast cancer. Ann Oncol. 2007;18:1591-1593.

43. Stelljes M, Strothotte R, Pauels H, et al. Graft-versus-host disease after allogeneic hematopoietic stem cell transplantation induces a CD8+ T cell-mediated graft-versus-tumor effect that is independent of the recognition of alloantigenic tumor targets. Blood. 2004;104:1210-1216.